

# Quantifying Statistical Significance of Neural Network-based Image Segmentation by Selective Inference

Vo Nguyen Le Duy

Nagoya Institute of Technology and RIKEN

duy.mllab.nit@gmail.com

Shogo Iwazaki

Nagoya Institute of Technology

iwazaki.s.nit@gmail.com

Ichiro Takeuchi

Nagoya Institute of Technology and RIKEN

takeuchi.ichiro@nitech.ac.jp

December 22, 2024

## Abstract

Although a vast body of literature relates to image segmentation methods that use deep neural networks (DNNs), less attention has been paid to assessing the statistical reliability of segmentation results. In this study, we interpret the segmentation results as hypotheses driven by DNN (called DNN-driven hypotheses) and propose a method by which to quantify the reliability of these hypotheses within a statistical hypothesis testing framework. Specifically, we consider a statistical hypothesis test for the difference between the object and background regions. This problem is challenging, as the difference would be falsely large because of the adaptation of the DNN to the data. To overcome this difficulty, we introduce a conditional selective inference (SI) framework—a new statistical inference framework for data-driven hypotheses that has recently received considerable attention—to compute exact (non-asymptotic) valid  $p$ -values for the segmentation results. To use the conditional SI framework for DNN-based segmentation, we develop a new SI algorithm based on the homotopy method, which enables us to derive the exact (non-asymptotic) sampling distribution of DNN-driven hypothesis. We conduct experiments on both synthetic and real-world datasets, through which we offer evidence that our proposed method can successfully control the false positive rate, has good performance in terms of computational efficiency, and provides good results when applied to medical image data.

# 1 Introduction

Image segmentation is a fundamental task in computer vision, and it has been widely applied in many areas. The goal of image segmentation is to assign a label to every pixel in an observed image, such that pixels with the same label share certain characteristics. Numerous image segmentation algorithms have been developed in the literature, such as thresholding [Otsu, 1979],  $k$ -means clustering [Dhanachandra et al., 2015], region-growing [Nock and Nielsen, 2004], and graph cuts [Boykov and Funka-Lea, 2006, Boykov and Jolly, 2001]. However, over the past few years, image segmentation using deep neural networks (DNNs) has become a new-generation model that exhibits remarkable performance improvements [Long et al., 2015, Badrinarayanan et al., 2017, Ronneberger et al., 2015].

Although a vast body of literature relates to DNN-based segmentation task methods, less attention has been paid to evaluating the statistical reliability of such segmentation results. In the absence of statistical reliability information, it is difficult to manage the risk of obtaining incorrect segmentation results. These false segmentation results can be harmful when they are used in high-stakes decision-making, such as medical diagnoses or automatic driving. Therefore, it is necessary to develop a *valid* statistical inference method for data-driven DNN-based segmentation results that can properly control the risk of obtaining false positives.

In this study, we interpret the segmentation results as hypotheses that are driven by DNN (called DNN-driven hypotheses) and employ a statistical hypothesis testing framework to quantify the reliability of DNN-based segmentation results. For example, in segmentation problems where an image is divided into object and background regions, we can quantify the reliability of the segmentation results based on the statistical significance of the difference in average pixel intensities between these two regions. Unfortunately, traditional statistical tests cannot be applied to this problem, because the hypothesis (segmentation result) itself is selected by the data. Traditional statistical tests are valid only when the hypothesis is predetermined independently of the data. Roughly speaking, if a hypothesis is selected by the data, the hypothesis will overfit the data; therefore, when assessing the reliability of the data-driven hypothesis, the bias needs to be properly corrected.

The main contribution of this study is that it introduces the *conditional selective inference (SI)* approach for testing the reliability of data-driven DNN-based segmentation. The basic idea behind conditional SI is to perform statistical inference under the condition that the hypothesis is selected. The conditional SI approach has been demonstrated as effective in the context of feature selection, such as in Lasso [Lee et al., 2016]. In this study, in order to introduce conditional SI for DNN-based segmentation, we develop a novel SI algorithm based on the homotopy method. This enables us to derive the exact (non-asymptotic) conditional sampling distribution of the DNN-driven hypothesis.

We use the  $p$ -value as a criterion to quantify the reliability of the segmentation results. In the

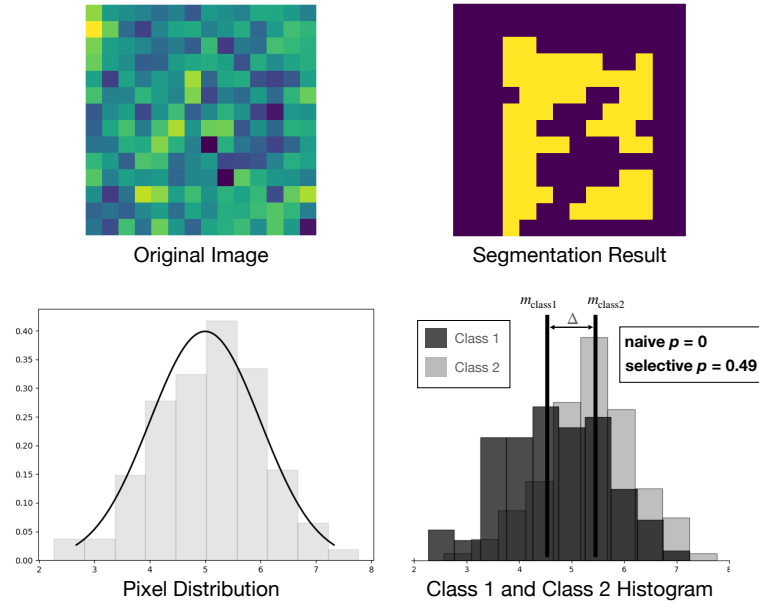


Figure 1: Illustration of segmentation bias and the importance of the proposed method. We generate a  $14 \times 14$  null image in which all the “true” pixel values are the same (upper-left). The lower-left plot shows the distribution of pixel values, and the upper-right plot shows the segmentation results obtained by a trained DNN. The lower-right plot shows histograms of the pixel intensities in the background region (Class 1) and object region (Class 2), as well as the naive  $p$ -value and the proposed selective  $p$ -value. Even from an image containing no specific objects, one can see that the pixel intensities between the object and background regions are clearly different. Therefore, the naive  $p$ -value is very small, indicating that it cannot be used to properly evaluate the reliability of the segmentation result. By applying the proposed method, we can successfully identify false segmentation result.

literature,  $p$ -values are often misinterpreted, and various sources of misinterpretation have been discussed [Wasserstein and Lazar, 2016]. However, in this study, by using conditional SI, we address one of the sources of misinterpreted  $p$ -values: the  $p$ -values are biased when the hypotheses are selected after looking at the data (often called double-dipping or data dredging). We believe that our approach is the first significant step toward providing *valid*  $p$ -values by which to assess the reliability of DNN-based segmentation. Figure 1 illustrates the bias inherent in a segmentation task in a simple simulation and shows the importance of our method.

## 1.1 Related works

In traditional statistical inference, a statistical model and statistical target are determined before looking at the data. Therefore, if we apply traditional methods to hypotheses selected after observing the

dataset, the inferential results are no longer valid, because *selection bias* exists. It can be interpreted that bias arises because the observed data are used twice: once for segmentation and once again for inference. This is often referred to as *double dipping* [Kriegeskorte et al., 2009]. In statistics, it has been recognized that naively computing  $p$ -values in double dipping is highly biased. Correcting this bias is challenging, especially when the hypotheses are selected using complicated procedures such as DNN.

In the past few years, conditional SI has been recognized as a new promising approach by which to evaluate the statistical reliability of data-driven hypotheses, and it has been actively studied for inference on the features of linear models selected by several feature selection methods—for example, Lasso [Lee et al., 2016, Liu et al., 2018, Le Duy and Takeuchi, 2021]. The basic idea of SI is to make inferences conditional on the selection event, which allows us to derive the exact (non-asymptotic) sampling distribution of the test statistic. In addition, SI has been applied to various problems [Bachoc et al., 2014, Fithian et al., 2015, Choi et al., 2017, Tian and Taylor, 2018, Chen and Bien, 2019, Hyun et al., 2018, Bachoc et al., 2018, Loftus and Taylor, 2014, Loftus, 2015, Panigrahi et al., 2016, Tibshirani et al., 2016, Yang et al., 2016, Suzumura et al., 2017, Duy et al., 2020, Sugiyama et al., 2021a, Tsukurimichi et al., 2021, Duy and Takeuchi, 2021, Das et al., 2021, Sugiyama et al., 2021b]. However, to the best of our knowledge, no study to date provides conditional SI for DNNs. This introduces additional technical difficulties.

The most closely related work (and the motivation for this study) is Tanizaki et al. [2020], where the authors provide a framework to compute valid  $p$ -values for image segmentation results obtained by graph cuts and threshold-based segmentation algorithms. The novel idea of Tanizaki et al. [2020] is to consider the sampling distribution of the test statistic conditional on the selection event, in which the segmentation result is obtained from the segmentation algorithm. In that study, since characterizing the necessary and sufficient selection event is intractable, the authors propose additionally conditioning on all the operations of the algorithm itself; in this way, the *over-conditioning* selection event is characterized by a set of quadratic inequalities. This suggests that the method is still valid—in the sense that the false positive rate (FPR) is properly controlled—but it has low statistical power because of over-conditioning. In addition, it is difficult to extend their approach to the case of segmentation using DNNs, because the selection event of DNN-based segmentation is much more complicated than that of graph cuts.

There are various types of DNN-based segmentation approaches; however, in this study, we focus on the most standard one, the supervised segmentation approach. In supervised segmentation, given a training set in the form of pairs of an image and its segmentation result annotated by domain specialists, a DNN is trained. In this study, our goal is to quantify the reliability of the segmentation

result when a new test image is given to the trained DNN in the aforementioned conditional SI framework.

## 1.2 Contribution

To the best of our knowledge, this is the first study to provide an *exact (non-asymptotic)* inference method for statistically quantifying the reliability of data-driven image segmentation results obtained from DNNs. We propose a novel *homotopy method*, inspired by Le Duy and Takeuchi [2021], to conduct a more powerful and efficient conditional SI for DNN-based segmentation tasks. We undertake experiments on both synthetic and real-world datasets, through which we offer evidence that our proposed method can successfully control the FPR, has good performance in terms of computational efficiency, and provides good results in practical applications.

## 2 Problem Statement

To formulate the problem, we denote an image with  $n$  pixels corrupted with Gaussian noise as

$$\mathbf{X} = (X_1, \dots, X_n)^\top = \boldsymbol{\mu} + \boldsymbol{\varepsilon}, \quad \boldsymbol{\varepsilon} \sim \mathbb{N}(\mathbf{0}, \Sigma), \quad (1)$$

where  $\boldsymbol{\mu} \in \mathbb{R}^n$  is an unknown mean pixel intensity vector, and  $\boldsymbol{\varepsilon} \in \mathbb{R}^n$  is a vector of normally distributed noise with covariance matrix  $\Sigma$ , which is known or can be estimated from external data. We note that the assumption in Equation (1) does not mean that the pixel intensities in an image follow a normal distribution. Instead, we assume that the vector of noise added to the true pixel values follows a multivariate normal distribution. Given a DNN that has already been trained in advance for the segmentation task, our target task is to quantify the statistical significance of the segmentation result obtained when applying the trained DNN to a new test input image  $\mathbf{X}$ .

For simplicity, we mainly focus on DNN-based segmentation problems in which the input image is divided into two regions. Nevertheless, the proposed method can be easily extended to cases where the image is divided into more than two regions. We call these two regions the *object* and *background* regions. We denote the set of pixels of an input image  $\mathbf{X}$  in the object and background regions as  $\mathcal{O}_{\mathbf{X}}$  and  $\mathcal{B}_{\mathbf{X}}$ , respectively.

### 2.1 Quantifying the statistical significance of the DNN-based segmentation result.

Given an observed image  $\mathbf{x}^{\text{obs}} \in \mathbb{R}^n$ , which is assumed to be sampled from model (1), we can obtain the object region  $\mathcal{O}_{\mathbf{x}^{\text{obs}}}$  and the background region  $\mathcal{B}_{\mathbf{x}^{\text{obs}}}$  after applying the trained DNN to  $\mathbf{x}^{\text{obs}}$ . To

quantify the statistical significance of the segmentation results, we consider the following statistical test.

$$H_0 : \mu_{\mathcal{O}_{\mathbf{x}^{\text{obs}}}} = \mu_{\mathcal{B}_{\mathbf{x}^{\text{obs}}}} \quad \text{vs.} \quad H_1 : \mu_{\mathcal{O}_{\mathbf{x}^{\text{obs}}}} \neq \mu_{\mathcal{B}_{\mathbf{x}^{\text{obs}}}}, \quad (2)$$

where  $\mu_{\mathcal{O}_{\mathbf{x}^{\text{obs}}}}$  and  $\mu_{\mathcal{B}_{\mathbf{x}^{\text{obs}}}}$  are the true means of the pixel values in the object and background regions, respectively. A reasonable choice of the test statistic is the difference in the average pixel values between the object and background regions.

$$\boldsymbol{\eta}^\top \mathbf{X} = \frac{1}{|\mathcal{O}_{\mathbf{x}^{\text{obs}}}|} \sum_{i \in \mathcal{O}_{\mathbf{x}^{\text{obs}}}} X_i - \frac{1}{|\mathcal{B}_{\mathbf{x}^{\text{obs}}}|} \sum_{i \in \mathcal{B}_{\mathbf{x}^{\text{obs}}}} X_i,$$

where  $\boldsymbol{\eta} \in \mathbb{R}^n$  is the vector indicating the test-statistic direction in the  $n$ -dimensional space, which is defined as

$$\boldsymbol{\eta} = \frac{1}{|\mathcal{O}_{\mathbf{x}^{\text{obs}}}|} \mathbf{1}_{\mathcal{O}_{\mathbf{x}^{\text{obs}}}}^n - \frac{1}{|\mathcal{B}_{\mathbf{x}^{\text{obs}}}|} \mathbf{1}_{\mathcal{B}_{\mathbf{x}^{\text{obs}}}}^n, \quad (3)$$

and  $\mathbf{1}_{\mathcal{C}}^n \in \mathbb{R}^n$  is a vector whose elements belonging to a set  $\mathcal{C}$  are set to 1, and 0 otherwise. Given a significance level  $\alpha \in [0, 1]$  (e.g., 0.05), we reject the null hypothesis  $H_0$  if the  $p$ -value is smaller than  $\alpha$ , which indicates that the object region differs from the background region. Otherwise, we cannot say that a difference is significant.

Suppose, for now, that the hypothesis in (2) is fixed—that is, nonrandom. Then, the naive (two-sided)  $p$ -value is simply given as

$$p_{\text{naive}} = \mathbb{P}_{H_0} (|\boldsymbol{\eta}^\top \mathbf{X}| \geq |\boldsymbol{\eta}^\top \mathbf{x}^{\text{obs}}|). \quad (4)$$

Given a significance level  $\alpha \in [0, 1]$ , because the hypothesis in (2) is assumed to be fixed,  $p_{\text{naive}}$  is valid in the sense that  $\mathbb{P}_{H_0}(p_{\text{naive}} < \alpha) = \alpha$ , that is,  $p_{\text{naive}}$  follows a uniform distribution between 0 and 1 under the null hypothesis. However, because the hypothesis in (2) is not fixed in advance, the naive  $p$ -value is *not valid* in the sense that, if we reject  $H_0$  with a significance level  $\alpha$ , the false detection rate (type-I error) cannot be controlled at level  $\alpha$ —that is, the distribution of  $p_{\text{naive}}$  under the null hypothesis is no longer uniform in  $[0, 1]$  (see Fig. 2a). Therefore, it is not possible to quantify the reliability of the data-driven segmentation results based on  $p_{\text{naive}}$ . This is due to the fact that the hypothesis in (2) is *selected* based on the data (the input image), and thus selection bias exists. This selection bias is sometimes called *data dredging*, *data snooping*, or *p-hacking* [Ioannidis, 2005, Head et al., 2015].

## 2.2 Conditional SI for computing valid $p$ -values

To properly address the selection bias, we employ conditional SI framework. The basic idea of conditional SI is to make inferences conditional on the selection event; this allows us to derive the *exact*

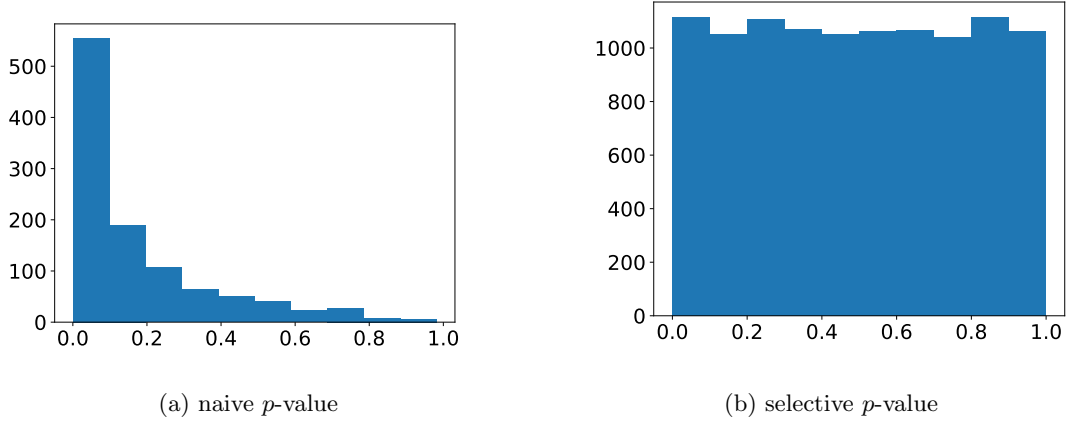


Figure 2: Distribution of the naive  $p$ -value and the selective  $p$ -value when hypotheses are selected based on the data (i.e., random) and the null hypothesis is true. It is obvious that the naive  $p$ -value does not follow a uniform distribution; this means that the naive  $p$ -value is unreliable, because it fails to control the FPR given the significance level  $\alpha \in [0, 1]$ . In contrast, the distribution of selective  $p$ -value is uniform. Therefore, the selective  $p$ -value is reliable because the FPR is properly controlled under  $\alpha$ .

(non-asymptotic) sampling distribution of the test statistic. Let us define  $\mathcal{A}(\mathbf{X})$  as an event in which the result of dividing the pixels of image  $\mathbf{X}$  into the object region  $\mathcal{O}_{\mathbf{X}}$  and the background region  $\mathcal{B}_{\mathbf{X}}$  is obtained by applying a trained DNN on  $\mathbf{X}$ —that is,

$$\mathcal{A}(\mathbf{X}) = \{\mathcal{O}_{\mathbf{X}}, \mathcal{B}_{\mathbf{X}}\}. \quad (5)$$

We consider the following sampling distribution of the test statistic  $\boldsymbol{\eta}^\top \mathbf{X}$  conditional on the segmentation results (i.e., selection event in which the object and background regions are identified)

$$\boldsymbol{\eta}^\top \mathbf{X} \mid \mathcal{A}(\mathbf{X}) = \mathcal{A}(\mathbf{x}^{\text{obs}}).$$

Then, to test the statistical significance of the segmentation result, we introduce the so-called (conditional) *selective  $p$ -value*  $p_{\text{selective}}$ , which satisfies the following sampling property:

$$\mathbb{P}_{H_0}(p_{\text{selective}} \leq \alpha \mid \mathcal{A}(\mathbf{X}) = \mathcal{A}(\mathbf{x}^{\text{obs}})) = \alpha, \quad (6)$$

that is,  $p_{\text{selective}}$  follows a uniform distribution under the null hypothesis (see Fig. 2b). We define the selective  $p$ -value as

$$p_{\text{selective}} = \mathbb{P}_{H_0}(|\boldsymbol{\eta}^\top \mathbf{X}| \geq |\boldsymbol{\eta}^\top \mathbf{x}^{\text{obs}}| \mid \mathcal{A}(\mathbf{X}) = \mathcal{A}(\mathbf{x}^{\text{obs}}), \mathbf{q}(\mathbf{X}) = \mathbf{q}(\mathbf{x}^{\text{obs}})), \quad (7)$$

where  $\mathbf{q}(\mathbf{X})$  is the nuisance parameter defined as

$$\mathbf{q}(\mathbf{X}) = (I_n - \mathbf{c}\boldsymbol{\eta}^\top)\mathbf{X} \quad \text{with} \quad \mathbf{c} = \Sigma\boldsymbol{\eta}(\boldsymbol{\eta}^\top\Sigma\boldsymbol{\eta})^{-1}.$$

Here, we would like to note that the selective  $p$ -value depends on  $\mathbf{q}(\mathbf{X})$ , but the sampling property in (6) continues to be satisfied without this additional condition because  $\mathbf{q}(\mathbf{X})$  is independent of the test statistic  $\boldsymbol{\eta}^\top \mathbf{X}$ . Under the assumption of Gaussian noise in (1), it is easy to confirm that this nuisance component is independent of  $\boldsymbol{\eta}^\top \mathbf{X}$ . The  $\mathbf{q}(\mathbf{X})$  corresponds to the component  $\mathbf{z}$  in the seminal conditional SI paper Lee et al. [2016] (see Section 5, Eq. 5.2 and Theorem 5.2). We note that additional conditioning on  $\mathbf{q}(\mathbf{X})$  is a standard approach in the conditional SI literature and is used in almost all the conditional SI-related studies cited in this paper.

### 2.3 Challenges in computing the selective $p$ -value

The discussion thus far indicates that we can conduct a valid and exact statistical inference for the DNN-based segmentation result if we can compute the selective  $p$ -value in (7). However, to compute  $p_{\text{selective}}$ , the major challenge is to characterize the selection event  $\mathcal{A}(\mathbf{X}) = \mathcal{A}(\mathbf{x}^{\text{obs}})$ . Most existing conditional SI studies consider the case in which the selection event is represented as an intersection of a set of linear or quadratic inequalities. For example, in the seminal work of conditional SI for Lasso [Lee et al., 2016], the selective  $p$ -value is computed by exploiting the fact that the event that some features (as well as their signs) selected by Lasso are represented as an intersection of a set of linear inequalities—that is, the selection event is represented as a polyhedron in the sample (data) space. Unfortunately, the selection event  $\mathcal{A}(\mathbf{X}) = \mathcal{A}(\mathbf{x}^{\text{obs}})$  in (7) is complicated because it is the selection event of the DNN, and it cannot be simply represented as an intersection of linear or quadratic inequalities. In addition, characterization of the selection event is also computationally challenging, as we need to identify the whole set of data with the same segmentation result as the observed data  $\mathbf{x}^{\text{obs}}$ . In the next section, we propose a novel method that addresses all the aforementioned challenges by utilizing the concept of a parametrized line search (i.e., the homotopy method).

## 3 Proposed Method

In this section, we propose a method for computing selective  $p$ -values. To obtain the selective  $p$ -value in (7), the main task is to identify the following set of  $\mathbf{x} \in \mathbb{R}^n$  that satisfies the condition part:

$$\mathcal{X} = \{\mathbf{x} \in \mathbb{R}^n \mid \mathcal{A}(\mathbf{x}) = \mathcal{A}(\mathbf{x}^{\text{obs}}), \mathbf{q}(\mathbf{x}) = \mathbf{q}(\mathbf{x}^{\text{obs}})\}. \quad (8)$$

To identify  $\mathcal{X}$ , we first reformulate the problem of identifying this conditional data space as a problem of searching the data on a parametrized line. In the following, we introduce a homotopy method to conduct a parametrized line search.

### 3.1 Characterization of the Conditional Data Space $\mathcal{X}$

According to the second condition  $\mathbf{q}(\mathbf{x}) = \mathbf{q}(\mathbf{x}^{\text{obs}})$  in (8), the data in  $\mathcal{X}$  are restricted to a line in  $\mathbb{R}^n$ , as stated in the following lemma.

**Lemma 1.** *Let us define*

$$\mathbf{a} = \mathbf{q}(\mathbf{x}^{\text{obs}}) \quad \text{and} \quad \mathbf{b} = \Sigma \boldsymbol{\eta} (\boldsymbol{\eta}^\top \Sigma \boldsymbol{\eta})^{-1}. \quad (9)$$

*Then, the conditional data space  $\mathcal{X}$  can be rewritten using a scalar parameter  $z \in \mathbb{R}$  as*

$$\mathcal{X} = \{\mathbf{x}(z) = \mathbf{a} + \mathbf{b}z \mid z \in \mathcal{Z}\}, \quad (10)$$

$$\text{where } \mathcal{Z} = \{z \in \mathbb{R} \mid \mathcal{A}(\mathbf{x}(z)) = \mathcal{A}(\mathbf{x}^{\text{obs}})\}. \quad (11)$$

*Proof.* According to the second condition in (8), we have

$$\begin{aligned} \mathbf{q}(\mathbf{x}) &= \mathbf{q}(\mathbf{x}^{\text{obs}}) \\ \Leftrightarrow \left( I_n - \mathbf{c} \boldsymbol{\eta}^\top \right) \mathbf{x} &= \mathbf{q}(\mathbf{x}^{\text{obs}}) \\ \Leftrightarrow \mathbf{x} &= \mathbf{q}(\mathbf{x}^{\text{obs}}) + \frac{\Sigma \boldsymbol{\eta}}{\boldsymbol{\eta}^\top \Sigma \boldsymbol{\eta}} \boldsymbol{\eta}^\top \mathbf{x}. \end{aligned}$$

By defining  $\mathbf{a} = \mathbf{q}(\mathbf{x}^{\text{obs}})$ ,  $\mathbf{b} = \Sigma \boldsymbol{\eta} (\boldsymbol{\eta}^\top \Sigma \boldsymbol{\eta})^{-1}$ ,  $z = \boldsymbol{\eta}^\top \mathbf{x}$ ,  $\mathbf{x}(z) = \mathbf{a} + \mathbf{b}z$ , and incorporating the first condition in (8), we obtain the result in Lemma 1.  $\blacksquare$

We note that while the seminal conditional SI work Lee et al. [2016] already implicitly exploits considerations of the data on the line, this was explicitly discussed for the first time in Section 6 of Liu et al. [2018]. Lemma 1 indicates that we need not consider the  $n$ -dimensional data space. Instead, we need only consider the *one-dimensional projected* data space  $\mathcal{Z}$  in (11). Now, let us consider a random variable  $Z \in \mathbb{R}$  and its observation  $z^{\text{obs}} \in \mathbb{R}$  that satisfies  $\mathbf{X} = \mathbf{a} + \mathbf{b}Z$  and  $\mathbf{x}^{\text{obs}} = \mathbf{a} + \mathbf{b}z^{\text{obs}}$ . Then, the selective  $p$ -value in (7) is rewritten as

$$\begin{aligned} p_{\text{selective}} &= \mathbb{P}_{H_0} (|\boldsymbol{\eta}^\top \mathbf{X}| \geq |\boldsymbol{\eta}^\top \mathbf{x}^{\text{obs}}| \mid \mathbf{X} \in \mathcal{X}) \\ &= \mathbb{P}_{H_0} (|Z| \geq |z^{\text{obs}}| \mid Z \in \mathcal{Z}). \end{aligned} \quad (12)$$

Because the variable  $Z \sim \mathbb{N}(0, \boldsymbol{\eta}^\top \Sigma \boldsymbol{\eta})$  under the null hypothesis,  $Z \mid Z \in \mathcal{Z}$  follows a *truncated* normal distribution. Once the truncation region  $\mathcal{Z}$  is identified, computation of the selective  $p$ -value in (12) is straightforward. Therefore, the remaining task is to identify  $\mathcal{Z}$ .

### 3.2 Identification of Truncation Region $\mathcal{Z}$

As discussed in §3.1, to calculate the selective  $p$ -value (12), we must identify the truncation region  $\mathcal{Z}$  in (11). To construct  $\mathcal{Z}$ , we must (a) compute  $\mathcal{A}(\mathbf{x}(z))$  for all  $z \in \mathbb{R}$ , and (b) identify the set

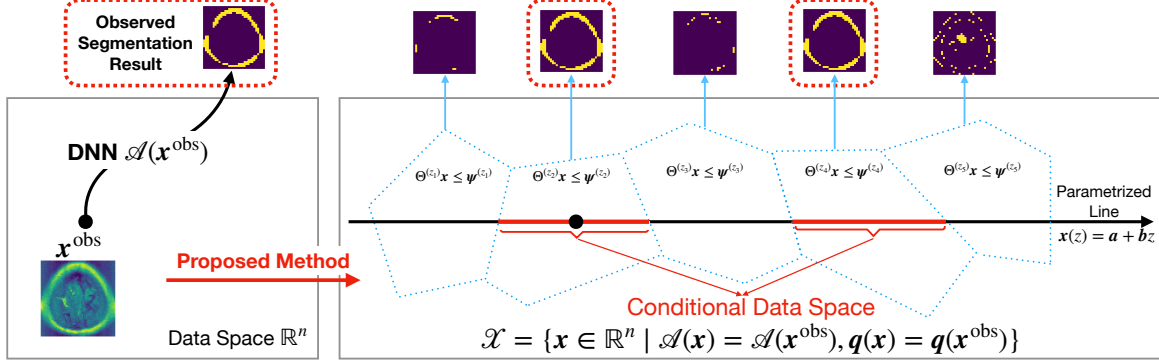


Figure 3: A schematic illustration of the proposed method. By applying DNN to the observed image  $\mathbf{x}^{\text{obs}}$ , we obtain a segmentation result. Then, we parametrize  $\mathbf{x}^{\text{obs}}$  with a scalar parameter  $z$  in the dimension of the test statistic to identify the subspace  $\mathcal{X}$  whose data have the *same* segmentation result as  $\mathbf{x}^{\text{obs}}$ . Finally, the valid statistical inference is conducted conditional on  $\mathcal{X}$ . We introduce a homotopy method for efficiently characterizing the conditional data space  $\mathcal{X}$ .

of intervals of  $z$  on which  $\mathcal{A}(\mathbf{x}(z)) = \mathcal{A}(\mathbf{x}^{\text{obs}})$ . However, it seems intractable to obtain  $\mathcal{A}(\mathbf{x}(z))$  for infinitely many values of  $z \in \mathbb{R}$ .

Our first idea in introducing SI for DNN is that we additionally condition some extra events to make the problem tractable. We now focus on a class of DNNs whose activation functions (AFs) are piecewise-linear—for example, ReLU, Leaky ReLU (the extension to general AFs is discussed later). Then, we consider additional conditioning on the selected piece of each piecewise-linear AF in the DNN.

**Definition 1.** Let  $s_j(\mathbf{x})$  be “the selected piece” of a piecewise-linear AF at the  $j$ -th unit in a DNN for a given input image  $\mathbf{x}$ , and let  $\mathbf{s}(\mathbf{x})$  be the set of  $s_j(\mathbf{x})$  for all the nodes in a DNN.

For example, given a ReLU AF,  $s_j(\mathbf{x})$  takes either 0 or 1, depending on whether the input to the  $j$ -th unit is located at the flat part (inactive) or the linear part (active) of the ReLU function. Using the notion of selected pieces  $\mathbf{s}(\mathbf{x})$ , instead of computing the selective  $p$ -value in (12), we consider the following *over-conditioning (oc)* conditional  $p$ -value:

$$p_{\text{selective}}^{\text{oc}} = \mathbb{P}_{H_0} (|Z| \geq |z^{\text{obs}}| \mid Z \in \mathcal{Z}^{\text{oc}}), \quad (13)$$

where  $\mathcal{Z}^{\text{oc}} = \{z \in \mathbb{R} \mid \mathcal{A}(\mathbf{x}(z)) = \mathcal{A}(\mathbf{x}^{\text{obs}}), \mathbf{s}(\mathbf{x}(z)) = \mathbf{s}(\mathbf{x}^{\text{obs}})\}$ . However, such an over-conditioning in SI leads to a loss of statistical power [Lee et al., 2016].

Our second idea is to develop a *homotopy method* to resolve the over-conditioning problem—that is, remove the conditioning of  $\mathbf{s}(\mathbf{x}(z)) = \mathbf{s}(\mathbf{x}^{\text{obs}})$ . Using the homotopy method, we can efficiently compute  $\mathcal{A}(\mathbf{x}(z))$  in a finite number of operations without the need to consider infinitely many values

of  $z \in \mathbb{R}$ , which is subsequently used to obtain the truncation region  $\mathcal{Z}$  in (11). The main idea is to compute a finite number of *breakpoints* at which one node of the network changes its status from active to inactive or vice versa. This concept is similar to the regularization path of Lasso, where we can compute a finite number of breakpoints at which the active set changes.

To this end, we introduce a two-step iterative approach, generally described as follows (see Fig. 3):

- **Step 1 (over-conditioning step).** Considering the over-conditioning case by additionally conditioning on the selected pieces of all hidden nodes in the DNN.
- **Step 2 (homotopy step).** Combining multiple over-conditioning cases using the homotopy method to obtain  $\mathcal{A}(\mathbf{x}(z))$  for all  $z \in \mathbb{R}$ .

### 3.3 Step 1: Over-conditioning Step

We now show that by additionally conditioning on the selected pieces  $\mathbf{s}(\mathbf{x}^{\text{obs}})$  of all the hidden nodes, we can write the selection event of the DNN as a set of linear inequalities.

**Lemma 2.** *Consider a class of DNN that consists of affine operations and piecewise-linear AFs. Then, the overconditioning region is written as*

$$\mathcal{Z}^{\text{oc}} = \{z \in \mathbb{R} \mid \Theta^{(\mathbf{s}(\mathbf{x}^{\text{obs}}))} \mathbf{x}(z) \leq \psi^{(\mathbf{s}(\mathbf{x}^{\text{obs}}))}\}$$

using a matrix  $\Theta^{(\mathbf{s}(\mathbf{x}^{\text{obs}}))}$  and a vector  $\psi^{(\mathbf{s}(\mathbf{x}^{\text{obs}}))}$  that depend only on the selected pieces  $\mathbf{s}(\mathbf{x}^{\text{obs}})$ .

*Proof.* For the class of DNN that consists of affine operations and piecewise-linear AFs, by fixing the selected pieces of all the piecewise-linear AFs, the input to each AF is represented by an affine function of an image  $\mathbf{x}$ . Therefore, the condition for selecting a piece in a piecewise-linear AF,  $s_j(\mathbf{x}(z)) = s_j(\mathbf{x}^{\text{obs}})$ , is written as a linear inequality with respect to  $\mathbf{x}(z)$ . ■

**Remark 1.** (Activation functions in the hidden layers) In this work, we focus mainly on a trained DNN where the AFs used at hidden layers are *piecewise linear*—for example, ReLU, Leaky ReLU, which is commonly used in a convolutional neural network (CNN). Otherwise, if there is any specific demand to use non-piecewise linear functions (such as sigmoid or hyperbolic tangent) in hidden layers, we can apply a piecewise-linear approximation approach to these functions. We provide examples of such approximation in Appendix C.

**Remark 2.** (Operations in a trained neural network) Most basic operations in a trained neural network are written as affine operations. In a traditional neural network, the multiplication results between the weight matrix and the output of the previous layer and its summation with the bias vector is an affine operation. In a CNN, the main convolution operation and upsampling operation

are obviously affine operations. Even when an operation in a DNN is NOT represented as a *single* affine operation, it is often the case that the operation is represented by as a *set* of affine operations, as in the following remark.

**Remark 3.** (Max-pooling operation) Although the max-pooling operation is not an affine operation, it can be written as a set of linear inequalities. For instance,  $v_1 = \max\{v_1, v_2, v_3\}$  can be written as a set  $\{e_1^\top \mathbf{v} \leq e_2^\top \mathbf{v}, e_1^\top \mathbf{v} \leq e_3^\top \mathbf{v}\}$ , where  $\mathbf{v} = (v_1, v_2, v_3)^\top$  and  $e_i$  is the standard basis vector with 1 at position  $i$ .

**Remark 4.** (Activation functions at the output layer) In Remark 1, we mention that we need to perform piecewise linear approximation for non-piecewise linear activations. However, if these functions are used at the output layer (e.g., sigmoid function or hyperbolic tangent function), we need *not* perform the approximation task, because we can define the set of linear inequalities based on the values prior to activation. See the next example for the case of a sigmoid function.

**Example 1.** Let us consider a three-layer neural network with  $n$  input nodes,  $h$  hidden nodes, and  $n$  output nodes. Let  $W^{(1)} \in \mathbb{R}^{h \times n}$  and  $\mathbf{w}^{(1)} \in \mathbb{R}^h$  be the weight matrix and bias vector between the input and hidden layers, respectively, and  $W^{(2)} \in \mathbb{R}^{n \times h}$  and  $\mathbf{w}^{(2)} \in \mathbb{R}^n$  be the weight matrix and bias vector between the hidden and output layers, respectively. The AF at the hidden layer is ReLU, and we use a sigmoid function at the output layer. At the hidden layer, for any node  $j \in [h]$ , the selection event is written as

$$\begin{cases} W_{j,:}^{(1)} \mathbf{x} + w_j^{(1)} \geq 0, & \text{if the output of ReLU function at } j^{\text{th}} \text{ node} \geq 0, \\ W_{j,:}^{(1)} \mathbf{x} + w_j^{(1)} < 0, & \text{otherwise,} \end{cases}$$

where the subscript  $j, :$  for a matrix indicates the  $j^{\text{th}}$  row of the matrix. Let  $\mathbf{a}^{(1)} \in \mathbb{R}^h$  and  $\mathbf{s}^{(1)} \in \mathbb{R}^h$  be the vectors in which  $a_{j \in [h]}^{(1)} = 1, s_{j \in [h]}^{(1)} = 1$  if the output of the ReLU function at the  $j^{\text{th}}$  node  $\geq 0$ , and  $a_j^{(1)} = 0, s_j^{(1)} = -1$  otherwise. Then we have the linear inequality system  $\Theta_1 \mathbf{x} \leq \psi_1$ , where  $\Theta_1 = (-s_1^{(1)} W_{1,:}^{(1)}, \dots, -s_h^{(1)} W_{h,:}^{(1)})^\top$  and  $\psi_1 = (s_1^{(1)} w_1^{(1)}, \dots, s_h^{(1)} w_h^{(1)})^\top$ . Next, for any output node  $o \in [n]$ , the selection event—a linear inequality—is written as

$$\begin{cases} W_{o,:}^{(2)} ((W^{(1)} \mathbf{x} + \mathbf{w}^{(1)}) \circ \mathbf{a}^{(1)}) + w_o^{(2)} \geq 0, & \text{if the output of sigmoid function} \geq 0.5, \\ W_{o,:}^{(2)} ((W^{(1)} \mathbf{x} + \mathbf{w}^{(1)}) \circ \mathbf{a}^{(1)}) + w_o^{(2)} < 0, & \text{otherwise,} \end{cases}$$

where  $\circ$  is the elementwise product. Similar to the hidden layer, we can construct the linear inequality system  $\Theta_2 \mathbf{x} \leq \psi_2$  at the output layer. Finally, the whole linear inequality system is written as

$$\Theta \mathbf{x} \leq \psi = (\Theta_1 \ \Theta_2)^\top \mathbf{x} \leq (\psi_1 \ \psi_2)^\top. \quad (14)$$

---

**Algorithm 1** `compute_solution_path`


---

**Input:**  $\mathbf{a}, \mathbf{b}, [z_{\min}, z_{\max}]$ 

- 1: Initialization:  $t = 1, z_t = z_{\min}, \mathcal{T} = z_t$
- 2: **while**  $z_t < z_{\max}$  **do**
- 3:   Compute the corresponding data  $\mathbf{x}(z_t) = \mathbf{a} + \mathbf{b}z_t$  in  $\mathbb{R}^n$  of  $z_t$
- 4:   Obtain  $\mathcal{A}(\mathbf{x}(z_t))$  by applying a trained DNN to  $\mathbf{x}(z_t)$
- 5:   Compute the next breakpoint  $z_{t+1} \leftarrow$  Equation (15).
- 6:    $\mathcal{T} = \mathcal{T} \cup \{z_{t+1}\}$ , and  $t = t + 1$
- 7: **end while**

**Output:**  $\{\mathcal{A}(\mathbf{x}(z_t))\}_{z_t \in \mathcal{T}}$ 


---

### 3.4 Step 2: Homotopy Step

We now introduce a homotopy method by which to compute  $\mathcal{A}(\mathbf{x}(z))$ , in which we combine multiple over-conditioning steps.

**Lemma 3.** *Consider a real value  $z_t$ . By applying a trained DNN to  $\mathbf{x}(z_t)$ , we obtain a set of linear inequalities  $\Theta^{(\mathbf{s}(\mathbf{x}(z_t)))}\mathbf{x}(z_t) \leq \psi^{(\mathbf{s}(\mathbf{x}(z_t)))}$ . Then, the next breakpoint  $z_{t+1} > z_t$ , at which the status of one node is changed from active to inactive or vice versa—that is, the sign of one linear inequality changes. This breakpoint is calculated by*

$$z_{t+1} = \min_{k: (\Theta^{(\mathbf{s}(\mathbf{x}(z_t)))}\mathbf{b})_k > 0} \frac{\psi_k^{(\mathbf{s}(\mathbf{x}(z_t)))} - (\Theta^{(\mathbf{s}(\mathbf{x}(z_t)))}\mathbf{a})_k}{(\Theta^{(\mathbf{s}(\mathbf{x}(z_t)))}\mathbf{b})_k}. \quad (15)$$

The proof of Lemma 3 is provided in Appendix A. Algorithm 1 shows our solution to efficiently identify  $\mathcal{A}(\mathbf{x}(z))$ . In this algorithm, multiple *breakpoints*  $z_1 < z_2 < \dots < z_{|\mathcal{T}|}$  are computed one by one. Each breakpoint  $z_t, t \in [|\mathcal{T}|]$  indicates the point at which the sign of one linear inequality is changed—that is, the status of one node in the network will change from active to inactive or vice versa. By identifying all these breakpoints  $\{z_t\}_{t \in [|\mathcal{T}|]}$ ,  $\mathcal{A}(\mathbf{x}(z))$  is given by

$$\mathcal{A}(\mathbf{x}(z)) = \begin{cases} \mathcal{A}(\mathbf{x}(z_1)) & \text{if } z \in [z_1 = z_{\min}, z_2], \\ \mathcal{A}(\mathbf{x}(z_2)) & \text{if } z \in [z_2, z_3], \\ \vdots & \\ \mathcal{A}(\mathbf{x}(z_{|\mathcal{T}|})) & \text{if } z \in [z_{|\mathcal{T}|}, z_{|\mathcal{T}|+1} = z_{\max}]. \end{cases}$$

Algorithm 2 shows the entire procedure for calculating the selective  $p$ -value in (12). First, we apply a DNN on  $\mathbf{x}^{\text{obs}}$  to obtain the observed segmentation result  $\mathcal{A}(\mathbf{x}^{\text{obs}})$ . Next, we calculate the direction of the test statistic  $\boldsymbol{\eta}$ , which is used to identify a parameterized line in  $\mathbb{R}^n$ . Then, we compute  $\mathcal{A}(\mathbf{x}(z))$

---

**Algorithm 2** parametric\_SI\_DNN

---

**Input:**  $\mathbf{x}^{\text{obs}}, [z_{\min}, z_{\max}]$ 

- 1: Obtain  $\mathcal{A}(\mathbf{x}^{\text{obs}})$  by applying the pretrained DNN to  $\mathbf{x}^{\text{obs}}$
- 2: Compute  $\boldsymbol{\eta} \leftarrow$  Equation (3), and then calculate  $\mathbf{a}$  and  $\mathbf{b} \leftarrow$  Equation (9)
- 3:  $\mathcal{A}(\mathbf{x}(z)) \leftarrow \text{compute\_solution\_path}(\mathbf{a}, \mathbf{b}, [z_{\min}, z_{\max}])$  // Algorithm 1
- 4: Identify truncation region  $\mathcal{Z} \leftarrow \{z : \mathcal{A}(\mathbf{x}(z)) = \mathcal{A}(\mathbf{x}^{\text{obs}})\}$
- 5:  $p_{\text{selective}} \leftarrow$  Equation (12)

**Output:**  $p_{\text{selective}}$ 

---

by using Algorithm 1. After obtaining  $\mathcal{A}(\mathbf{x}(z))$ , we identify  $\mathcal{Z}$  in (11), which is the key factor for computing the selective  $p$ -value.

**Choice of**  $[z_{\min}, z_{\max}]$ . Under a normal distribution, neither very positive nor very negative  $z$  values affect the inference. Therefore, it is reasonable to consider a range of values—for example,  $[-20\sigma, 20\sigma]$  Liu et al. [2018], where  $\sigma$  is the standard deviation of the sampling distribution of the test statistic.

## 4 Experiment

In this section, we demonstrate the performance of the proposed method.

### 4.1 Methods for comparison

We compare the *proposed method* (homotopy method), which is the main focus of this paper, with the following approaches:

- *Proposed-method-oc (over-conditioning):* This is our first idea of characterizing the conditional data space by additionally conditioning on the observed activeness and inactiveness of all the nodes. The major limitation of this method is its low statistical power due to over-conditioning. The over-conditioning selective  $p$ -value is computed by (13).
- *Naive method:* This method uses the classical  $z$ -test to calculate the naive  $p$ -value in (4).
- *Permutation test:* This too is a well-known technique for computing the  $p$ -value. The permutation testing procedure is described as follows:
  - Compute the observed test statistic  $T^{\text{obs}}$  by applying the trained DNN on  $\mathbf{x}^{\text{obs}}$
  - For  $1 \leftarrow b$  to  $B$  ( $B$  is the number of permutations which is given by user)

- +  $\mathbf{x}^{(b)} \leftarrow \text{permute}(\mathbf{x}^{\text{obs}})$
- + Compute  $T^{(b)}$  by applying the trained DNN on  $\mathbf{x}^{(b)}$
- Compute the  $p$ -value as follows:

$$p_{\text{permutation}} = \frac{1}{B} \sum_{b=1}^B \mathbb{1}\{|T^{\text{obs}}| \leq |T^{(b)}|\}.$$

## 4.2 Experimental setup

Regarding the FPR experiments, we generate 120 null images.  $\mathbf{x} = (x_1, \dots, x_n)$  in which  $x_i \in [n] \sim N(0, 1)$  for each  $n \in \{16, 64, 256, 1024\}$ . For each  $n$  value, we run 120 trials. To test the power, we generate images  $\mathbf{x} = (x_1, \dots, x_n)$  with  $n = 256$ , in which the *true* average difference in the underlying model  $\mu_{\mathcal{O}_x} - \mu_{\mathcal{B}_x} = \Delta_\mu \in \{0.5, 1.0, 1.5, 2.0\}$ . For each  $\Delta_\mu$  value, we run 120 trials. Since we conduct statistical testing only when there is a segmentation result discovered by the DNNs, we define the power as follows.

$$\text{Power} = \frac{\# \text{ detected \& rejected}}{\# \text{ detected}}.$$

This definition of power is the same as that in Hyun et al. [2018] and Duy et al. [2020], where  $\# \text{ detected}$  is the number of images on which a segmentation result is obtained by the trained DNN and  $\# \text{ rejected}$  is the number of images whose null hypothesis is rejected by our proposed method. We select the significance level  $\alpha = 0.05$ , and we use a CNN with the following structure:

Layer	Output Size
Input	$\sqrt{n} \times \sqrt{n} \times 1$
Conv (3, 3, 1, 4) <sup>a</sup>	$\sqrt{n} \times \sqrt{n} \times 4$
Max pooling	$\sqrt{n}/2 \times \sqrt{n}/2 \times 4$
Upsampling	$\sqrt{n} \times \sqrt{n} \times 4$
Conv (3, 3, 1, 1)	$\sqrt{n} \times \sqrt{n} \times 1$
Output	$\sqrt{n} \times \sqrt{n} \times 1$

<sup>a</sup> Conv([filter height], [filter width], [# channel], [# filter]).

In the DNN literature, scholars propose many new network architectures for segmentation problems, one after another [Long et al., 2015, Ronneberger et al., 2015, Badrinarayanan et al., 2017]. Although these new DNN architectures for segmentation often have a very complex structure, if they are broken down into smaller elements, each can often be represented (or at least well approximated) as an affine operation whose selection event can be handled by the proposed method. Because the main contribution of this study is its introduction of a conditional SI framework by which to evaluate

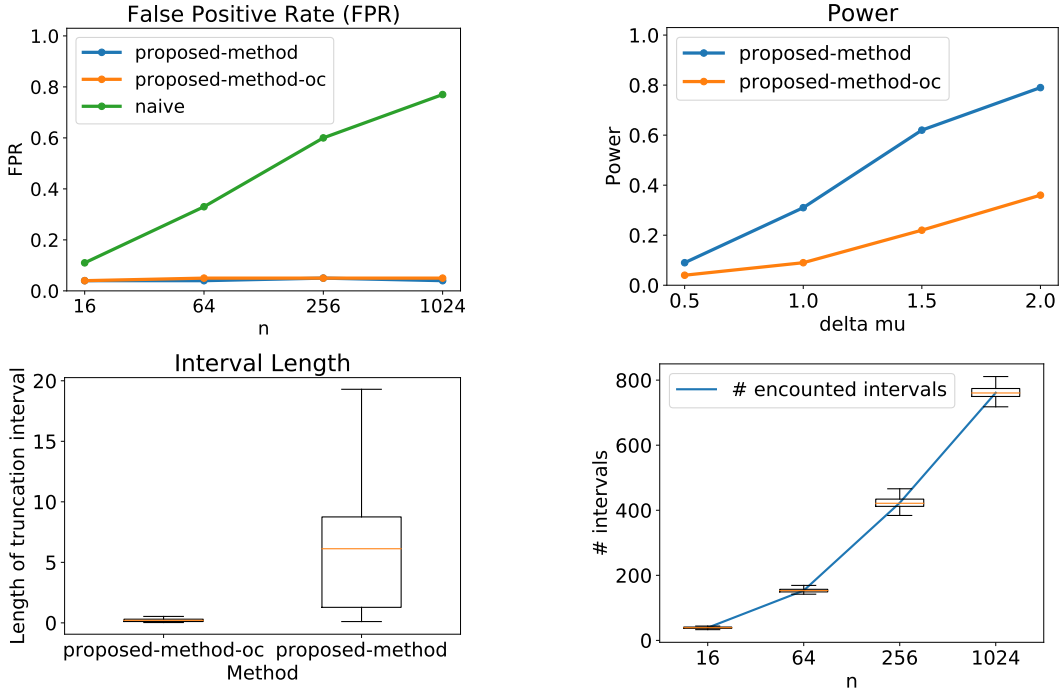


Figure 4: Results of false positive rate, power, interval length, and encountered intervals.

the reliability of DNN-based segmentation, empirical implementations and evaluations of the newest complex DNN architectures are beyond the scope of this study.

### 4.3 Numerical results

The results of the FPR control are shown in the upper-left plot of Fig. 4. The proposed methods successfully control the FPR while the naive method *cannot*. Because the naive method fails to control the FPR, we no longer consider the power. In the upper-right plot of Fig. 4, the over-conditioning option has a lower power than the homotopy method. This is because the truncation region in the proposed-method-oc (over-conditioning) is shorter than that in the proposed method (homotopy), as shown in the lower-left plot of Fig. 4. The lower-right plot of Fig. 4 shows why the proposed homotopy method is efficient. Intuitively, to overcome the over-conditioning issue, we need to consider all combinations of the activenesses of the nodes in a trained DNN, which is exponentially increasing. With the homotopy method, we need only consider the number of encountered intervals on the line along the direction of the test statistic, which is almost linearly increasing in practice.

Additionally, we confirm the robustness of the proposed method in terms of FPR control by applying our method to data following Laplace distribution, skew normal distribution (skewness coefficient 10), and  $t_{20}$  distribution. We also consider the case where variance is also estimated from the data.

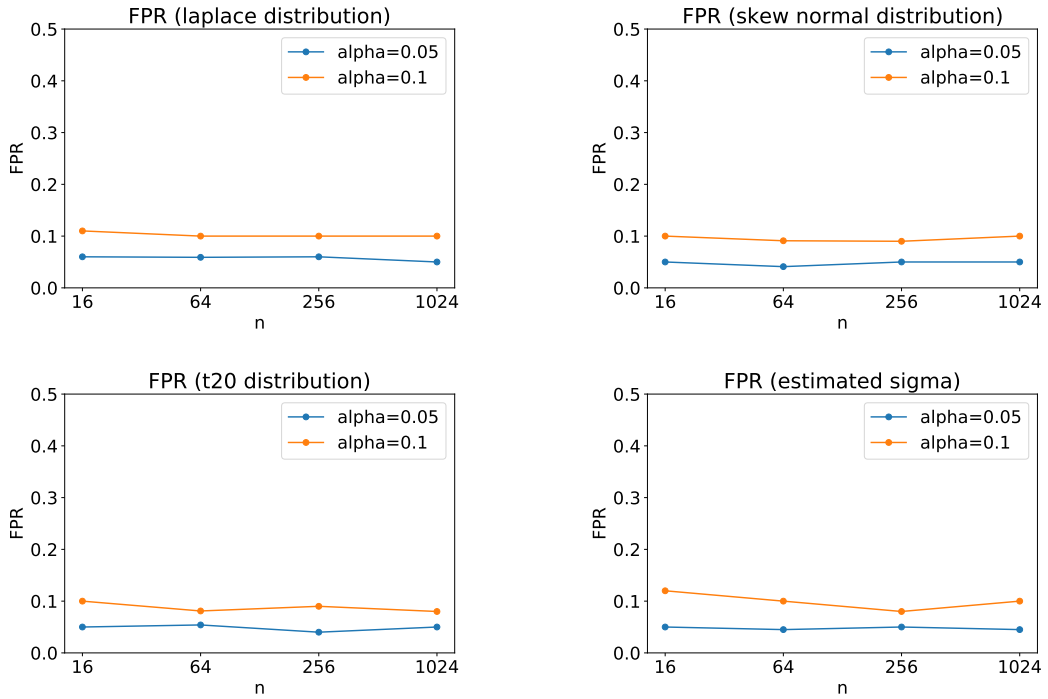


Figure 5: False positive rate of the proposed method when data are nonnormal or  $\sigma^2$  is unknown.

We test the FPR for both  $\alpha = 0.05$  and  $\alpha = 0.1$ . The FPR results are shown in Fig. 5. Our method still maintains good performance with regard to FPR control.

#### 4.4 Real-data examples

We examine the brain image dataset extracted from the dataset used by Buda et al. [2019], which includes 939 images with tumors and 941 images without tumors. We first compare our method to a permutation test in terms of FPR control. The results are shown in Table 1. Because the permutation test cannot properly control the FPR (i.e., the permutation test is unreliable), a comparison of power is no longer needed. Comparisons of the naive  $p$ -value and the selective  $p$ -value are shown in Fig. 6 and Fig. 7. The naive  $p$ -value remains small, even when the image has no tumor region; this indicated that naive  $p$ -values cannot be used to quantify the reliability of DNN-based segmentation results. The proposed method successfully identifies false positive and true positive detections.

## 5 Discussion

We propose a novel method by which to conduct statistical inference on the significance of the data-driven image segmentation result obtained by a trained DNN based on the concept of conditional

Table 1: False positive rate and power comparisons in a real-world brain image dataset.

	FPR	Power
Proposed Method	0.057	0.683
Permutation Test	0.640	-

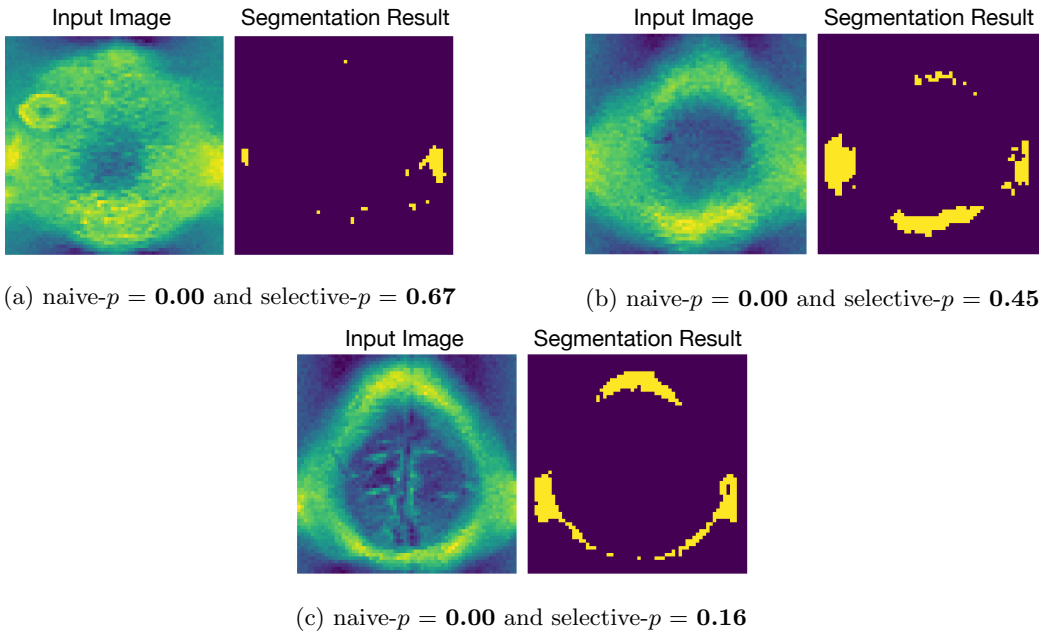


Figure 6: Inference on segmentation results for images without a tumor region.

SI. In the context of DNN-based image segmentation, we are primarily interested in the reliability of a trained network when given new inputs (i.e., not training inputs). Therefore, the validity of our proposed method is not contingent on DNN training.

We believe that this study stands as a significant step toward reliable artificial intelligence and opens several directions for statistically evaluating the reliability of DNN-driven hypotheses. Some open questions remain, as follows.

- The proposed method currently does not support a DNN with a softmax operator. Although the softmax operator can in theory be approximated by affine operations, doing so will be challenging in reality, as we need to work in a multidimensional space. Although it is difficult to apply the proposed method to network architectures containing components that are difficult to decompose into affine operations, one possible solution to this issue is to devise a new network architecture that can be

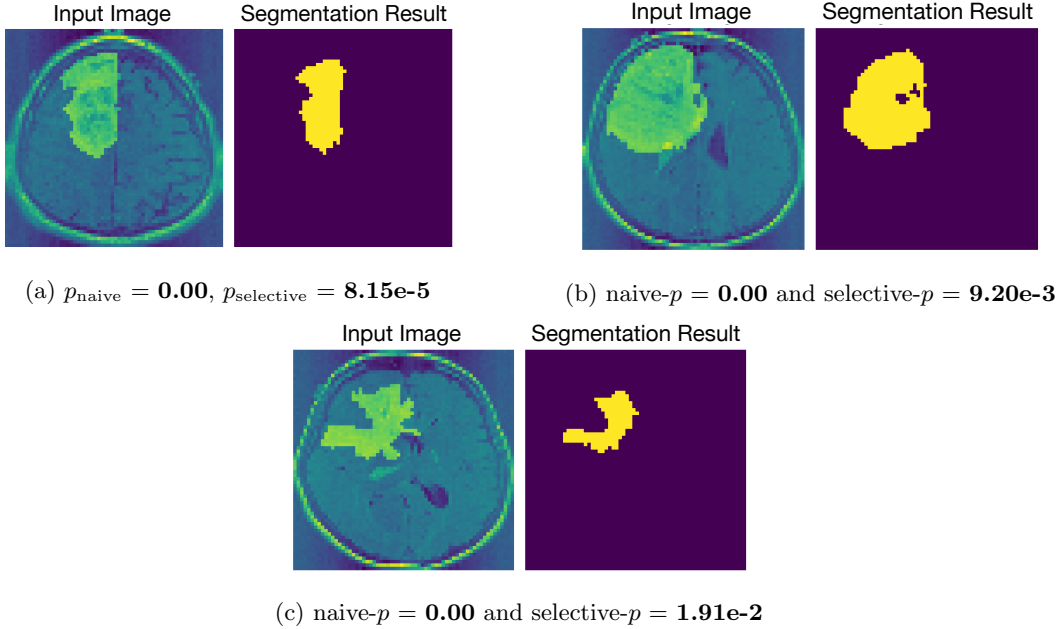


Figure 7: Inference on segmentation results for images where there exists a tumor region.

expressed as a set of affine functions but still has state-of-the-art segmentation performance.

- Although this study mainly focuses on the image segmentation task, the proposed method can be applied to a class of problems where (1) the test statistic is defined as a linear contrast with respect to the data and (2) the operations of the trained neural network can be characterized by a set of linear inequalities (or approximated by piecewise-linear functions). Therefore, widening the applicability of the proposed method to other computer vision tasks—as well as to other fields such as natural language processing and signal processing—would also stand as a valuable future contribution.

## Acknowledgements

This work was partially supported by MEXT KAKENHI (20H00601, 16H06538), JST CREST (JP-MJCR21D3), JST Moonshot R&D (JPMJMS2033-05), NEDO (JPNP18002, JPNP20006), RIKEN Center for Advanced Intelligence Project, and RIKEN Junior Research Associate Program.

## References

F. Bachoc, H. Leeb, and B. M. Pötscher. Valid confidence intervals for post-model-selection predictors. *arXiv preprint arXiv:1412.4605*, 2014.

F. Bachoc, G. Blanchard, and P. Neuvial. On the post selection inference constant under restricted isometry properties. *Electronic Journal of Statistics*, 12(2):3736–3757, 2018.

V. Badrinarayanan, A. Kendall, and R. Cipolla. Segnet: A deep convolutional encoder-decoder architecture for image segmentation. *IEEE transactions on pattern analysis and machine intelligence*, 39(12):2481–2495, 2017.

Y. Boykov and G. Funka-Lea. Graph cuts and efficient nd image segmentation. *International journal of computer vision*, 70(2):109–131, 2006.

Y. Y. Boykov and M.-P. Jolly. Interactive graph cuts for optimal boundary & region segmentation of objects in nd images. In *Proceedings eighth IEEE international conference on computer vision. ICCV 2001*, volume 1, pages 105–112. IEEE, 2001.

M. Buda, A. Saha, and M. A. Mazurowski. Association of genomic subtypes of lower-grade gliomas with shape features automatically extracted by a deep learning algorithm. *Computers in biology and medicine*, 109:218–225, 2019.

S. Chen and J. Bien. Valid inference corrected for outlier removal. *Journal of Computational and Graphical Statistics*, pages 1–12, 2019.

Y. Choi, J. Taylor, and R. Tibshirani. Selecting the number of principal components: Estimation of the true rank of a noisy matrix. *The Annals of Statistics*, 45(6):2590–2617, 2017.

D. Das, V. N. L. Duy, H. Hanada, K. Tsuda, and I. Takeuchi. Fast and more powerful selective inference for sparse high-order interaction model. *arXiv preprint arXiv:2106.04929*, 2021.

N. Dhanachandra, K. Manglem, and Y. J. Chanu. Image segmentation using k-means clustering algorithm and subtractive clustering algorithm. *Procedia Computer Science*, 54:764–771, 2015.

V. N. L. Duy and I. Takeuchi. More powerful conditional selective inference for generalized lasso by parametric programming. *arXiv preprint arXiv:2105.04920*, 2021.

V. N. L. Duy, H. Toda, R. Sugiyama, and I. Takeuchi. Computing valid p-value for optimal changepoint by selective inference using dynamic programming. In *Advances in Neural Information Processing Systems*, pages 11356–11367, 2020.

W. Fithian, J. Taylor, R. Tibshirani, and R. Tibshirani. Selective sequential model selection. *arXiv preprint arXiv:1512.02565*, 2015.

M. L. Head, L. Holman, R. Lanfear, A. T. Kahn, and M. D. Jennions. The extent and consequences of p-hacking in science. *PLoS Biol*, 13(3):e1002106, 2015.

S. Hyun, K. Lin, M. G’Sell, and R. J. Tibshirani. Post-selection inference for changepoint detection algorithms with application to copy number variation data. *arXiv preprint arXiv:1812.03644*, 2018.

J. P. Ioannidis. Why most published research findings are false. *PLoS medicine*, 2(8):e124, 2005.

N. Kriegeskorte, W. K. Simmons, P. S. Bellgowan, and C. I. Baker. Circular analysis in systems neuroscience: the dangers of double dipping. *Nature neuroscience*, 12(5):535–540, 2009.

V. N. Le Duy and I. Takeuchi. Parametric programming approach for more powerful and general lasso selective inference. In *International Conference on Artificial Intelligence and Statistics*, pages 901–909. PMLR, 2021.

J. D. Lee, D. L. Sun, Y. Sun, and J. E. Taylor. Exact post-selection inference, with application to the lasso. *The Annals of Statistics*, 44(3):907–927, 2016.

K. Liu, J. Markovic, and R. Tibshirani. More powerful post-selection inference, with application to the lasso. *arXiv preprint arXiv:1801.09037*, 2018.

J. R. Loftus. Selective inference after cross-validation. *arXiv preprint arXiv:1511.08866*, 2015.

J. R. Loftus and J. E. Taylor. A significance test for forward stepwise model selection. *arXiv preprint arXiv:1405.3920*, 2014.

J. Long, E. Shelhamer, and T. Darrell. Fully convolutional networks for semantic segmentation. In *Proceedings of the IEEE conference on computer vision and pattern recognition*, pages 3431–3440, 2015.

R. Nock and F. Nielsen. Statistical region merging. *IEEE Transactions on pattern analysis and machine intelligence*, 26(11):1452–1458, 2004.

N. Otsu. A threshold selection method from gray-level histograms. *IEEE transactions on systems, man, and cybernetics*, 9(1):62–66, 1979.

S. Panigrahi, J. Taylor, and A. Weinstein. Bayesian post-selection inference in the linear model. *arXiv preprint arXiv:1605.08824*, 28, 2016.

O. Ronneberger, P. Fischer, and T. Brox. U-net: Convolutional networks for biomedical image segmentation. In *International Conference on Medical image computing and computer-assisted intervention*, pages 234–241. Springer, 2015.

K. Sugiyama, V. N. L. Duy, and I. Takeuchi. More powerful and general selective inference for stepwise feature selection using the homotopy continuation approach. In *Proceedings of the 38th International Conference on Machine Learning*, 2021a.

R. Sugiyama, H. Toda, V. N. L. Duy, Y. Inatsu, and I. Takeuchi. Valid and exact statistical inference for multi-dimensional multiple change-points by selective inference. *arXiv preprint arXiv:2110.08989*, 2021b.

S. Suzumura, K. Nakagawa, Y. Umezawa, K. Tsuda, and I. Takeuchi. Selective inference for sparse high-order interaction models. In *Proceedings of the 34th International Conference on Machine Learning-Volume 70*, pages 3338–3347. JMLR. org, 2017.

K. Tanizaki, N. Hashimoto, Y. Inatsu, H. Hontani, and I. Takeuchi. Computing valid p-values for image segmentation by selective inference. In *Proceedings of the IEEE/CVF Conference on Computer Vision and Pattern Recognition*, pages 9553–9562, 2020.

X. Tian and J. Taylor. Selective inference with a randomized response. *The Annals of Statistics*, 46(2):679–710, 2018.

R. J. Tibshirani, J. Taylor, R. Lockhart, and R. Tibshirani. Exact post-selection inference for sequential regression procedures. *Journal of the American Statistical Association*, 111(514):600–620, 2016.

T. Tsukurimichi, Y. Inatsu, V. N. L. Duy, and I. Takeuchi. Conditional selective inference for robust regression and outlier detection using piecewise-linear homotopy continuation. *arXiv preprint arXiv:2104.10840*, 2021.

R. L. Wasserstein and N. A. Lazar. The asa statement on p-values: context, process, and purpose, 2016.

F. Yang, R. F. Barber, P. Jain, and J. Lafferty. Selective inference for group-sparse linear models. In *Advances in Neural Information Processing Systems*, pages 2469–2477, 2016.

## A Proof of Lemma 3

Given a real value  $z_t$ , we can always obtain  $\Theta^{(\mathbf{s}(\mathbf{x}(z_t)))}\mathbf{x}(z_t) \leq \psi^{(\mathbf{s}(\mathbf{x}(z_t)))}$  when applying the trained neural network on  $\mathbf{x}(z_t)$ . Then, for any  $z \in \mathbb{R}$ , if  $\Theta^{(\mathbf{s}(\mathbf{x}(z_t)))}\mathbf{x}(z) \leq \psi^{(\mathbf{s}(\mathbf{x}(z_t)))}$ ,  $\mathcal{A}(z_t) = \mathcal{A}(z)$  and  $\mathbf{s}(z_t) = \mathbf{s}(z)$ . By decomposing  $\mathbf{x}(z) = \mathbf{a} + \mathbf{b}z$ , we have

$$\begin{aligned} \{\Theta^{(\mathbf{s}(\mathbf{x}(z_t)))}\mathbf{x}(z) \leq \psi^{(\mathbf{s}(\mathbf{x}(z_t)))}\} &= \{\Theta^{(\mathbf{s}(\mathbf{x}(z_t)))}(\mathbf{a} + \mathbf{b}z) \leq \psi^{(\mathbf{s}(\mathbf{x}(z_t)))}\} \\ &= \{\Theta^{(\mathbf{s}(\mathbf{x}(z_t)))}\mathbf{b}z \leq \psi^{(\mathbf{s}(\mathbf{x}(z_t)))} - \Theta^{(\mathbf{s}(\mathbf{x}(z_t)))}\mathbf{a}\} \\ &= \{(\Theta^{(\mathbf{s}(\mathbf{x}(z_t)))}\mathbf{b})_k z \leq \psi_k^{(\mathbf{s}(\mathbf{x}(z_t)))} - (\Theta^{(\mathbf{s}(\mathbf{x}(z_t)))}\mathbf{a})_k \text{ for all } k\}. \end{aligned}$$

Then, the breakpoint  $z_{t+1} > z_t$  at which one node changes its status, i.e., the sign of one inequality is going to be changed, is computed as

$$z_{t+1} = \min_{k: (\Theta(\mathbf{s}(\mathbf{x}(z_t))) \mathbf{b})_k > 0} \frac{\psi_k^{(\mathbf{s}(\mathbf{x}(z_t)))} - (\Theta(\mathbf{s}(\mathbf{x}(z_t))) \mathbf{a})_k}{(\Theta(\mathbf{s}(\mathbf{x}(z_t))) \mathbf{b})_k}.$$

Hence, we have the result of Lemma 3.

## B Distribution of naive $p$ -value and selective $p$ -value when the null hypothesis is true

We demonstrate the validity of our proposed method by confirming the uniformity of  $p$ -value when the null hypothesis is true. We generated 12,000 null images  $\mathbf{x} = (x_1, \dots, x_n)$  in which  $x_i \in [n] \sim \mathbb{N}(0, 1)$  for each case  $n \in \{16, 64, 256\}$  and performed the experiments to check the distribution of naive  $p$ -values and selective  $p$ -values. From Figure 8, it is obvious that naive  $p$ -value does not follow uniform distribution. Therefore, it fails to control the false positive rate. The empirical distributions of selective  $p$ -value are shown in Figure 9. The results indicate our proposed method successfully controls the false detection probability.

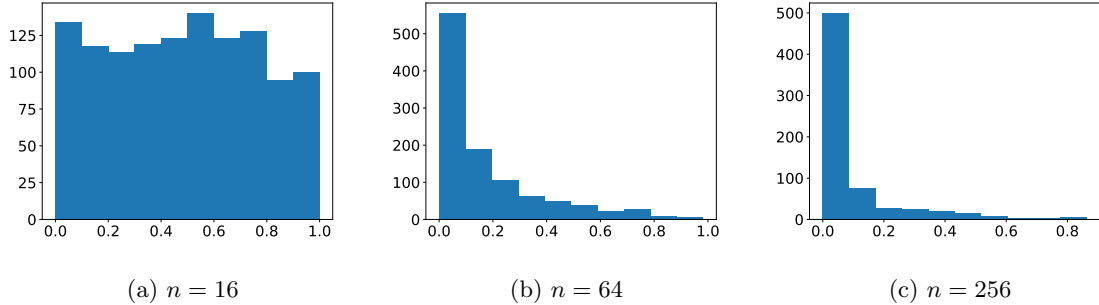


Figure 8: Distribution of naive  $p$ -value when the null hypothesis is true.

## C Examples of piecewise linear linear approximation for non-piecewise linear activation functions.

For simplicity, we consider a simple 3-layer neural network where the activation function at hidden layer is either sigmoid or tanh, the number of input nodes and output nodes are 8, and the number of hidden nodes is 16. Since these functions are non-piecewise linear functions, then we can use the

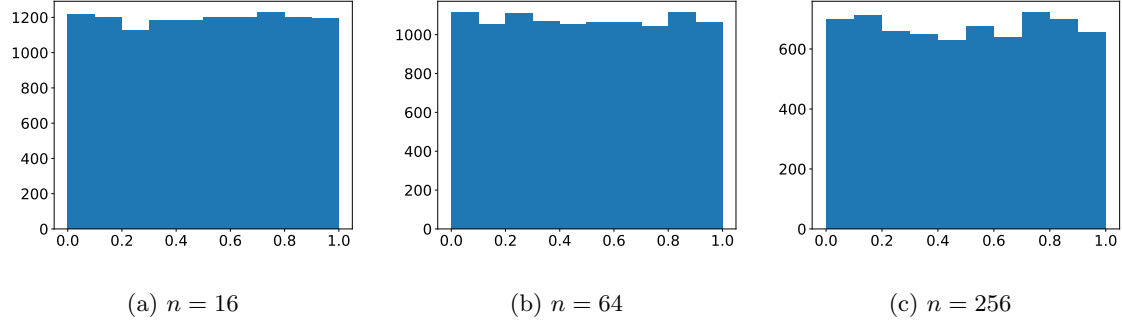


Figure 9: Distribution of selective  $p$ -value when the null hypothesis is true.

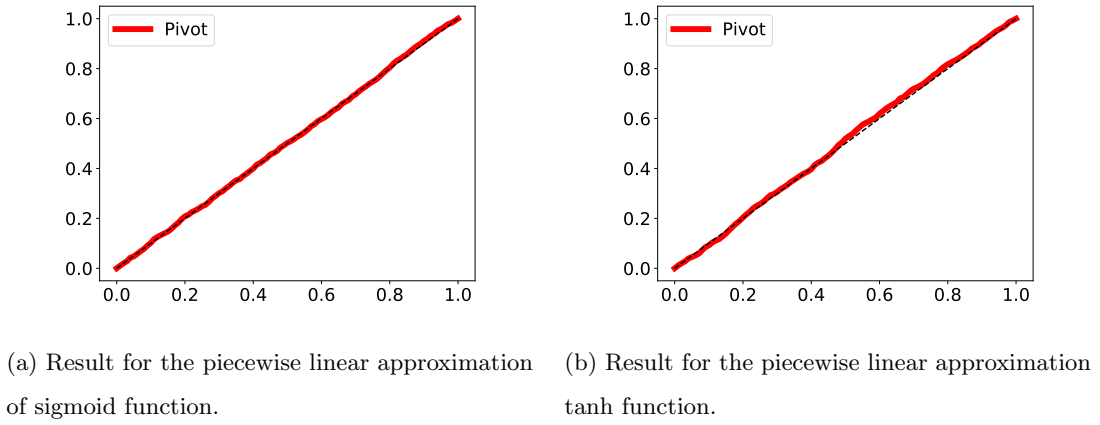


Figure 10: Uniform QQ-plot of the pivot.

following approximation

$$f(x) = \text{sigmoid}(x) = \begin{cases} 0 & \text{if } x < -4, \\ \frac{1}{8}x + \frac{1}{2} & \text{if } -4 \leq x \leq 4, \\ 1 & \text{if } x > 4. \end{cases}$$

$$f(x) = \tanh(x) = \begin{cases} -1 & \text{if } x < -2, \\ \frac{1}{2}x & \text{if } -2 \leq x \leq 2, \\ 1 & \text{if } x > 2. \end{cases}$$

With the above approximations, we demonstrate that our method still can control the FPR by showing the uniform QQ-plot of the pivot, which is the  $p$ -value under the null hypothesis, in Figure 10.

In the above example, we used 3 cuts (pieces) to approximate the function. Theoretically, when we increase # cuts, the number of encountered intervals tend to exponentially increase. However, in Figure 11, we show that # encountered intervals still linearly increase in practice.

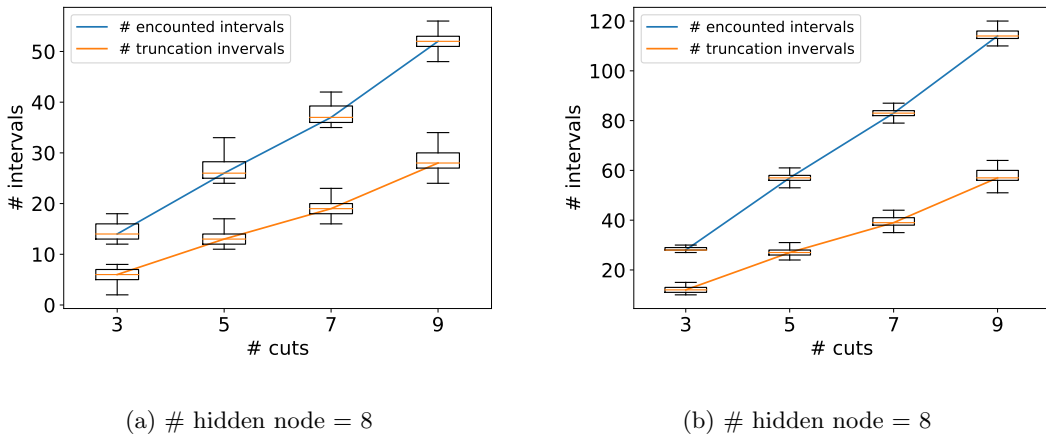


Figure 11: Demonstration of  $\#$  encountered and  $\#$  truncation intervals when increasing  $\#$  cuts (pieces).